

(Supporting Information)

## Electrochemical Reduction of CO<sub>2</sub> to CO by Heterogeneous Catalyst of Fe-Porphyrin-Based Metal-Organic Framework

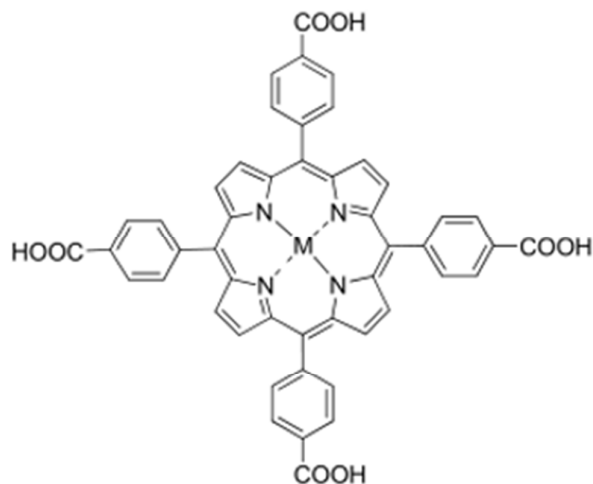
*Bao-Xia Dong,\* She-Liang Qian, Fan-Yan Bu, Yi-Chen Wu, Li-Gang Feng,  
Yun-Lei Teng,\* Wen-Long Liu, Zong-Wei Li*

School of Chemistry and Chemical Engineering, Yangzhou University, Yangzhou, 225002, P. R. China. Fax: E-mail: [bxdong@yzu.edu.cn](mailto:bxdong@yzu.edu.cn) (B-X. Dong); [ylteng@yzu.edu.cn](mailto:ylteng@yzu.edu.cn) (Y.-L. Teng)

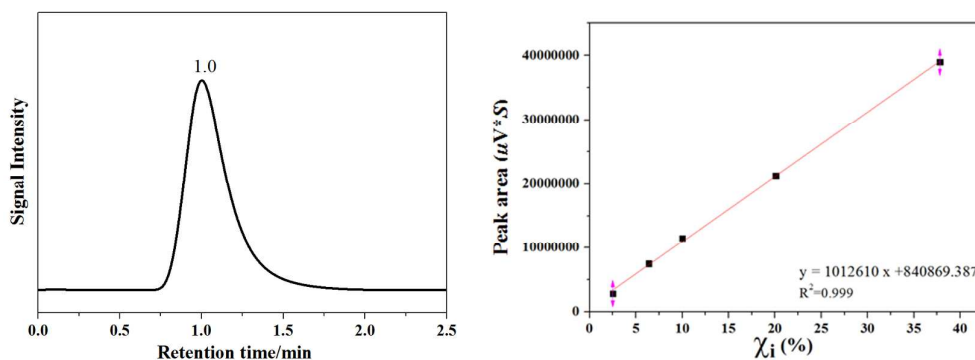
### Contents:

1. **Figure S1.** The molecular structure of the Fe-TCPP ligand.
2. **Figure S2.** Chromatographic peak (left) and standard curve (right) for pure hydrogen established on TDX-01 column for GC analysis.
3. **Figure S3.** Chromatographic peak (left) and standard curve (right) for pure CO established on TDX-01 column for GC analysis.
4. **Figure S4.** (a) Chromatographic peaks for pure methanol (2.2 min) and ethanol (2.4 min), as well as standard curves for methanol (b) and ethanol (c) established on PEG-20M column for GC analysis (n-propanol as internal standard).
5. **Figure S5.** Chromatographic peaks (a) and standard curve (b) for COOH<sup>-</sup> established on high-end ion chromatography.
6. **Figure S6.** IR spectra for PCN-222(Fe) and Fe-TCPP.
7. **Figure S7.** Normalized UV-vis spectra of pure TCPP-Fe and PCN-222(Fe) in CH<sub>2</sub>Cl<sub>2</sub> which show a Soret band at 444 nm.
8. **Figure S8.** CVs of PCN-222 (Fe)/C in CO<sub>2</sub>-saturated electrolyte. Insert shows the total charge integrated from the Fe<sup>III/II</sup> reduction wave ( $\Gamma = 1.622 \times 10^{-8} \text{ mol cm}^{-2}$ ).
9. **Table S1.** Performance of a selection of existing electrocatalysts
10. **Figure S9.** CVs of bare CP electrode, carbon black loaded on CP electrode and PCN-222 (Fe)/C loaded on CP in CO<sub>2</sub>-saturated electrolyte in the potential range -1.4~1.2 V vs RHE.
11. **Figure S10.** CVs of precursor of Fe-TCCP ligand ( $\Gamma = 2.89 \times 10^{-9} \text{ mol cm}^{-2}$ ), and PCN-222 (Fe)/C loaded on CP in CO<sub>2</sub>-saturated electrolyte in the potential range -0.5~0.8 V vs RHE.
12. **Table S2.** Summary of the chronoamperograms experiment parameters
13. **Figure S11.** Plot of  $\log(I_{\text{CO}})$  vs  $\eta$  for CO production at varying potential, Tafel slope: 188 mV/decade.

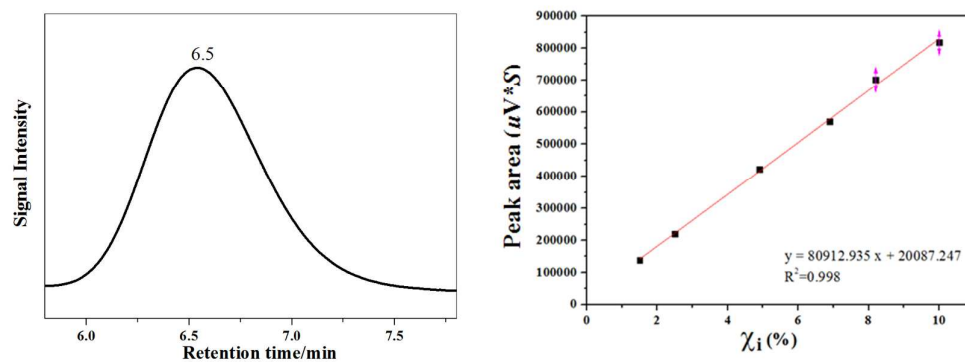
- 14. Figure S12.** Current density recorded for 2 h electrolyses (left) and FE analyses (right) at  $-0.60$  V vs RHE using carbon black, Fe-TCPP/C and PCN-222 (Fe)/C, respectively, loaded on CP in  $\text{CO}_2$ -saturated  $0.5$  M  $\text{KHCO}_3$ .
- 15. Table S3.** List of the chronoamperograms experiment parameters for catalysts with different PCN-222(Fe): C ratios
- 16. Figure S13.** SEM images of the PCN-222(Fe)/C composite electrode before and after electrolysis in a side view (a) and top-view (b, c), respectively.
- 17. Figure S14.** Fe2p core level spectra for as-synthesized PCN-222(Fe) and PCN-222(Fe)/C electrode loaded on carbon paper before and after electrolysis at  $-0.60$  V vs RHE for 2 h.
- 18. Figure S15.** Cl2p core level spectra for as-synthesized PCN-222(Fe) and PCN-222(Fe)/C electrode loaded on carbon paper before and after electrolysis at  $-0.60$  V vs RHE for 2 h.
- 19. Figure S16.** C1s core level spectra for as-synthesized PCN-222(Fe) and PCN-222(Fe)/C electrode loaded on carbon paper before and after electrolysis at  $-0.60$  V vs RHE for 2 h.
- 20. Figure S17.** N1s core level spectra for as-synthesized PCN-222(Fe) and PCN-222(Fe)/C electrode loaded on carbon paper before and after electrolysis at  $-0.60$  V vs RHE for 2 h.



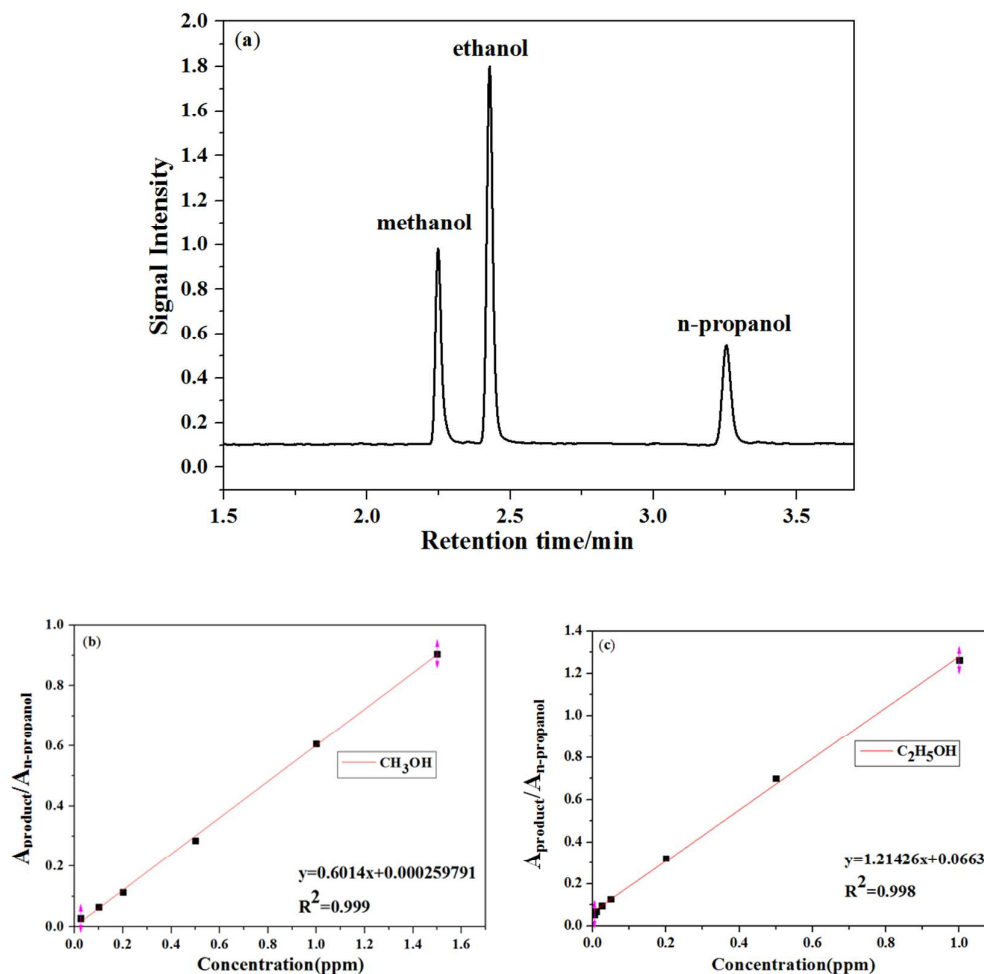
**Figure S1.** The molecular structure of the Fe-TCPP ligand.



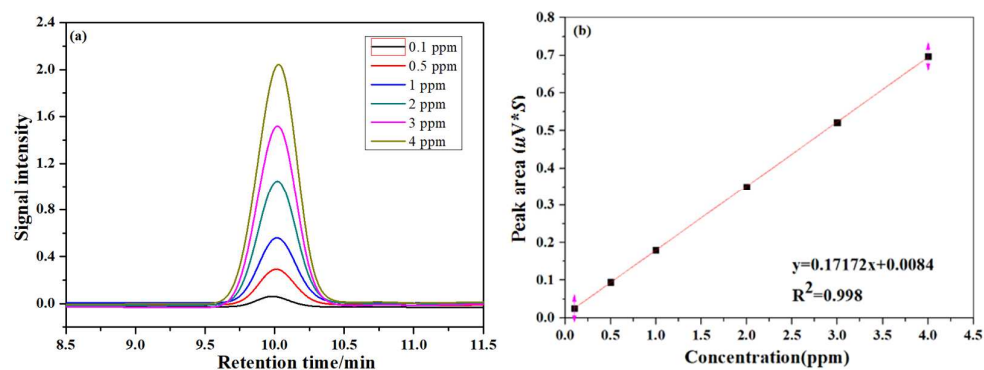
**Figure S2.** Chromatographic peak (left) and standard curve (right) for pure hydrogen established on TDX-01 column for GC analysis.



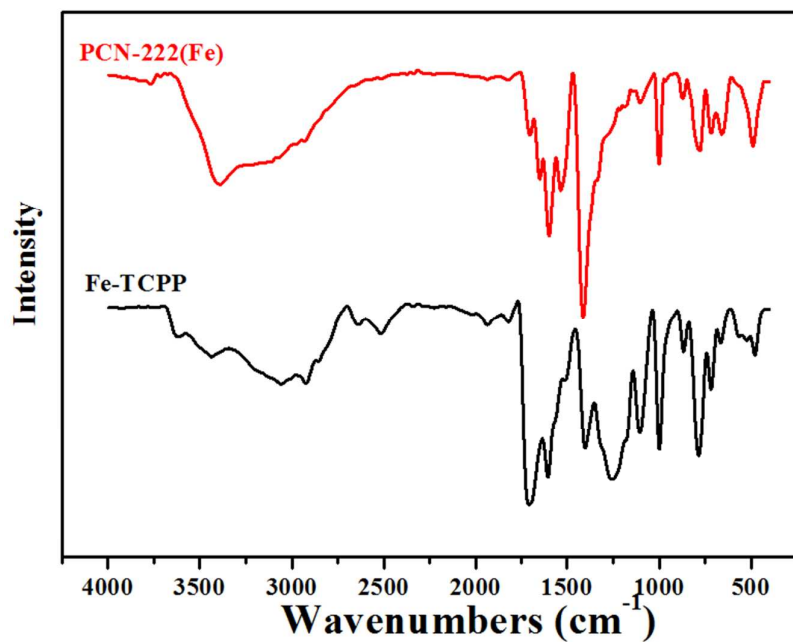
**Figure S3.** Chromatographic peak (left) and standard curve (right) for pure CO established on TDX-01 column for GC analysis.



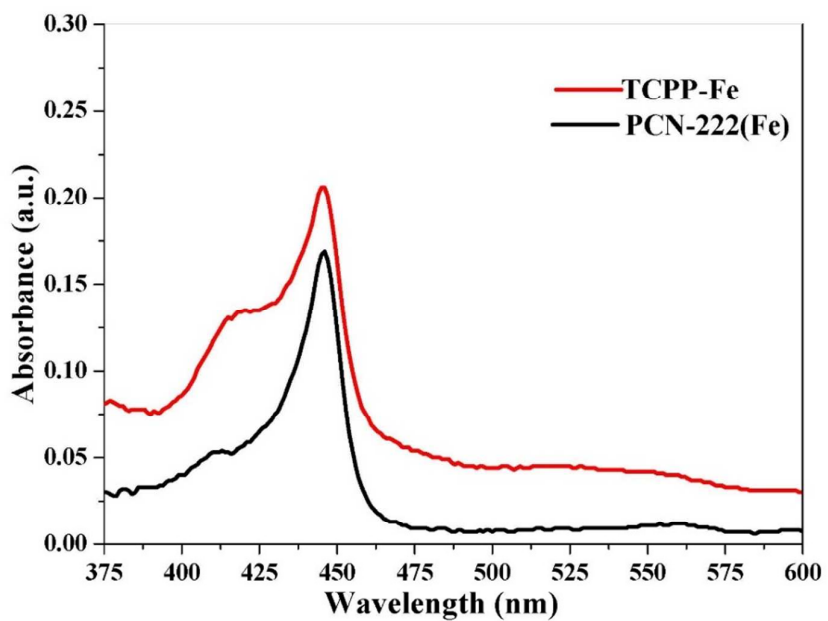
**Figure S4.** (a) Chromatographic peaks for pure methanol (2.2 min) and ethanol (2.4 min), as well as standard curves for methanol (b) and ethanol (c) established on PEG-20M column for GC analysis (n-propanol as internal standard).



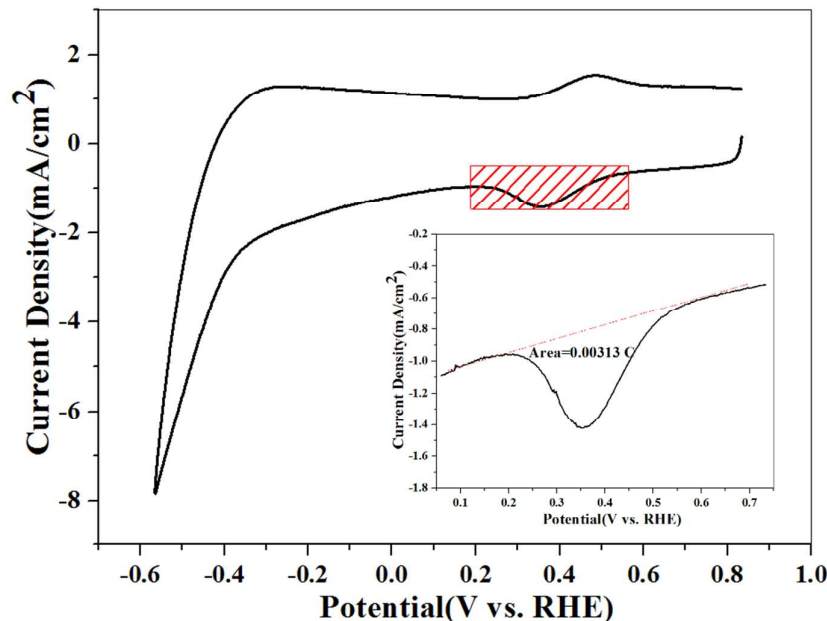
**Figure S5.** Chromatographic peaks (a) and standard curve (b) for  $\text{COOH}^-$  established on high-end ion chromatography.



**Figure S6.** IR spectra for PCN-222(Fe) and Fe-TCPP.



**Figure S7.** Normalized UV-vis spectra of pure TCPP-Fe and PCN-222(Fe) in CH<sub>2</sub>Cl<sub>2</sub> which show a Soret band at 444 nm.



**Figure S8.** CVs of PCN-222 (Fe)/C in CO<sub>2</sub>-saturated electrolyte. Insert shows the total charge integrated from the Fe<sup>III/II</sup> reduction wave ( $\Gamma = 1.622 \times 10^{-8} \text{ mol cm}^{-2}$ ).

**Calculation of the surface concentration of electrochemically active PCN-222(Fe) sites.** Integration of the peak area under the Fe<sup>III/II</sup> reduction wave leads to the charge that passed to reduce Fe(III) to Fe(II),  $Q_{CV} = 0.00313 \text{ C}$ . The surface concentration,  $\Gamma$ , is calculated using the following equation:  $\Gamma = Q_{CV}/nFA$  (1). Here,  $n$  is the number electrons transferred for the redox couple ( $n=1$ ),  $F$  is the Faraday constant, and  $A$  is the surface area of the electrode. It gives surface concentration of electroactive PCN-222(Fe):  $\Gamma = 1.622 \times 10^{-8} \text{ mol cm}^{-2}$ .

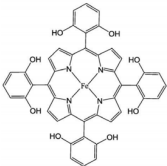

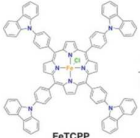
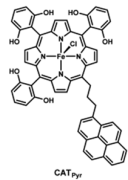
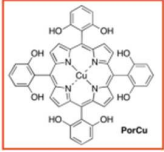
The amount of surface-active PCN-222 (Fe) sites is calculated by assuming a one-electron redox process:  $n = Q/F = 3.2 \times 10^{-8} \text{ mol}$ .

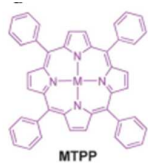
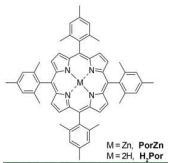
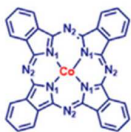
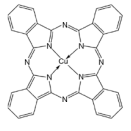
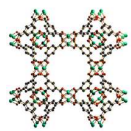
The total amount of PCN-222 (Fe) is calculated as follows:  $n_{\text{total}} = m/M = 2.0/2571.5 = 7.8 \times 10^{-7} \text{ mol}$ .

Then, the surface fraction of electrochemically active PCN-222 (Fe) sites is determined as follows:

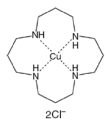
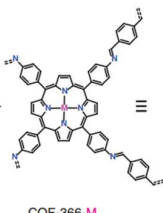
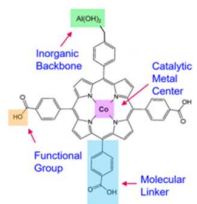
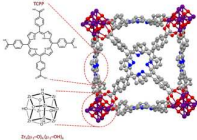
$$\chi = n/n_{\text{total}} = 4.17\%$$

**Table S1.** Performance of a selection of existing electrocatalysts

Catalyst	Electrolyte	Product	Potential [overpotential]/V	$J / \text{mA cm}^{-2}$	FE %	TOF/ molecules $\cdot \text{site}^{-1} \cdot \text{s}^{-1}$	TOF/ $\text{s}^{-1}$	$I \times 10^{-8} /$ mol $\text{cm}^{-2}$	Ref
PCN-222(Fe)	0.5 M $\text{KHCO}_3$	CO	−0.60 V vs RHE [0.494]	1.15	91	$0.336^{\text{M1}}$	$0.014_{\text{M1}}$	1.622	This work
					80.4	$0.286^{\text{M1}}$	$0.012_{\text{M1}}$		
<b>FeTDHPP</b> 	DMF+2 M $\text{H}_2\text{O}$	CO	−1.16 V vs NHE [0.47]	0.31	94	n.r.	11	n.r.	(1)
CoFPc (perfluorinated cobalt phthalocyanine) 	0.5 M $\text{NaHCO}_3$	CO	−0.80 V vs RHE [0.68]	~4.2	93	1.61	$0.13 \sim 2.1^{\text{M1}}$	1.3	(2)
Carbazole-functionlised <b>FeTCPP</b> 	0.1 M $\text{Bu}_4\text{NBF}_4/\text{dichloromethane}$	CO	n.r.	n.r.	n.r.	n.r.	n.r.	0.023	(3)
<b>CAT<sub>pyr</sub>-CNT</b> 	0.5 M $\text{NaHCO}_3$	CO	−1.03 V vs NHE [0.48]	~0.6	93	0.04	$0.04^{\text{M1}}$	$0.1 \sim 2.5$	(4)
<b>PorCu</b> 	0.5 M $\text{NaHCO}_3$	CO	−0.676 V vs RHE	~1	10	n.r.	n.r.	n.r.	(5)
		$\text{CH}_4$	−0.976 V vs RHE	~13.2	27	$4.3^{\text{M2}}$			
		$\text{C}_2\text{H}_4$	−0.976 V vs RHE	~8.4	17	$1.8^{\text{M2}}$		n.r.	
Co-TPP-CNT	0.5 M $\text{KHCO}_3$	CO	−1.15 V vs SCE [0.35]	0.59	83	n.r.	n.r.	17	(6)

 <p>MTPP</p>			-1.35 V vs SCE [0.55]	3.2	91		0.078 <sub>M1</sub>		
Fe-TPP-CNT	0.5 M KHCO <sub>3</sub>	CO	-1.35 V vs SCE [0.55]	0.9	64	n.r.	n.r.	n.r.	
<p>PorZn</p>  <p>M = Zn, PorZn M = Zn, H<sub>2</sub>Por</p>	0.1 M TBAPF <sub>6</sub> /DMF/ H <sub>2</sub> O	CO	-1.7 V vs SHE	2.1	95	14.4 <sup>M2</sup>		n.r.	(7)
Co-Pc/CNT (2.5%)	0.5 M KHCO <sub>3</sub>	CO	-0.63 V vs RHE [0.51]	10	92	2.7 <sup>M2</sup>		n.r.	
Co-Pc-CN/CNT (3.5%)	0.5 M KHCO <sub>3</sub>	CO	-0.63 V vs RHE [0.51]	15	98	4.1 <sup>M2</sup>		n.r.	(8)
	0.5 M KHCO <sub>3</sub>	CO	-0.46 V vs RHE [0.34]	5.6	88	1.4 <sup>M2</sup>		n.r.	
<p>CoPPc/CNT</p> 	0.5 M NaHCO <sub>3</sub>	CO	-0.61 V vs RHE [0.50]	20	90	1.36 <sup>M3</sup>		n.r.	(9)
<p>Cu-Pc</p> 	0.5 M KHCO <sub>3</sub>	CH <sub>4</sub>	-1.06 V vs RHE [0.94]	13	66	0.39 <sup>M4</sup>			(10)
<p>HKUST-1</p> 		CH <sub>4</sub>	-1.16 V vs RHE [1.04]	4.4	27	n.r.	n.r.		



<p>[Cu(cyclam)]Cl<sub>2</sub></p> 		CH <sub>4</sub>	-1.26 V vs RHE [1.14]	2.8	15	n.r.	n.r.		
<p>COF-366-Co</p> 	0.5 M KHCO <sub>3</sub>	CO	-0.67 V vs RHE [0.55]	1.8	90	0.69 <sup>M2</sup>	0.027 <sup>M2</sup>	1	(11)
<p>[Al<sub>2</sub>(OH)<sub>2</sub>TCPP-Co]MOF (TCPP-Co)</p> 	0.5 M KHCO <sub>3</sub>	CO	-0.7 V vs RHE [0.58]	1	76	0.056 <sup>M2</sup>		11	(12)
<p>Fe_MOF-525</p> 	1 M TBAPF <sub>6</sub> /CH <sub>3</sub> CN	CO	-1.3 V vs NHE [0.65]	2.3	54	0.018 <sup>M5</sup>		6.2	(13)
<p>n.r.—not reported</p> <p>M1-M5: different methods for calculating the TOF, as illustrated in the following context.</p>									

### About the calculation of the turnover number (TON) and turnover frequency (TOF) in the heterogeneous catalysis:

#### Method 1:

TON is defined as the total moles of carbon product formed ( $n_{\text{prod}}$ ) divided by total moles of catalyst employed in the electrolysis ( $n_{\text{cat}}$ ):  $\text{TON} = n_{\text{prod}}/n_{\text{cat}}$  (2)

TOF is defined as TON per unit time:  $\text{TOF} = \text{TON}/t = n_{\text{prod}}/(n_{\text{cat}}t)$  (3), where  $t$  is the electrolysis time.<sup>11</sup>

**We use this method for evaluating the catalysts in this work.**

#### Method 2:

The electrochemical double-layer (EDL) capacitance can be calculated by the equation below:  $C = i/v$  (4), where  $i$  is the current (mA) and  $v$  is the scan rate (mV s<sup>-1</sup>). The EDL capacitance, based on the CV measurements in the CO<sub>2</sub> saturated solution, could be derived from the slope of the

linear regression in the current-scan rate plot. TOF can be calculated by the equation:  $\text{TOF} = j/nem = kj/nCV$  (5), where  $j$  is the partial current (mA) resulting from CO production,  $n$  is the number of electrons transferred to produce one CO molecule ( $n=2$ ),  $e$  is the elementary charge ( $1.602 \times 10^{-19}$  C),  $m$  is the actual number of the exposed catalyst molecules,  $k$  is the number of elementary charges adsorbed on each molecule,  $C$  is the EDL capacitance (mF) and  $V$  is the potential window (V) of the CV measurements. Assuming one exposed catalyst molecule contributes to the EDL capacitance by adsorbing one elementary charge (e.g. a  $\text{K}^+$  ion), we have  $k=1$  and the TOFs for  $\text{CO}_2$ -to-CO conversion can be calculated.<sup>7</sup>

### Method 3:

TOF is defined as the mole of reduction product generated per electrocatalytic active site per unit time. Assuming that all catalyst sites are involved in the  $\text{CO}_2$  reduction reaction electrocatalysis:

$$\text{TOF} = j_{\text{tot}} \times FE_{\text{CO}} / 2F \times n_{\text{tot}} \quad (6)$$

In reality, only surface catalyst sites are involved in  $\text{CO}_2$  reduction reaction electrocatalysis. The corrected TOF is defined as follows:  $\text{TOF}_{\text{corrected}} = \text{TOF}/f$  (7), where  $f$  is the surface fraction of electrochemically active catalyst sites ( $f = n/n_{\text{tot}}$ ).

TON is defined as the mole of reduction product generated per electrocatalytic active site over a given period of time.

$\text{TON} = Q \times FE_{\text{CO(average)}} / 2F \times n_{\text{tot}}$  (8), where  $Q$  is the total reduction charge pass during the bulk electrocatalysis, and  $FE_{\text{CO(average)}}$  is the estimated average CO faradaic efficiency during the bulk electrocatalysis.<sup>9</sup>

When normalized to the number of electrocatalytically active catalyst sites on the surface:  $\text{TON}_{\text{corrected}} = \text{TON}/f$  (9).

### Method 4:

To calculate the TOF for the CuPc catalyst, the number of surface sites was estimated based on the size and geometry of the metallic Cu clusters using the equation below:

$$\mu = MN = M \frac{\alpha m N_A}{M_{\text{CuPc}}} \quad (10)$$

where  $\mu$  denotes the number of surface sites,  $M$  denotes the percentage of surface Cu atoms in a Cu clusters,  $N$  denotes the total number of Cu atoms in all the Cu clusters on the electrode,  $\alpha$  denotes the percentage of CuPc molecules that have restructured to Cu clusters,  $m$  denotes the original mass loading of CuPc ( $60 \mu\text{g cm}^{-2}$ ),  $N_A$  denotes the Avogadro constant, and  $M_{\text{CuPc}}$  denotes the molecular mass of CuPc ( $576.07 \text{ g mol}^{-1}$ ). Here,  $\alpha=80\%$  based on the XAS results. Consider that the Cu clusters are 2 nm cuboctahedra containing 162 surface Cu atoms and a total of 309 Cu atoms,  $M=0.524$ . Consequently,  $\mu=2.63 \times 10^{16}$  sites per  $\text{cm}^2$ . TOF was calculated using the equation below:

$$\text{TOF} = \frac{j}{ne\mu} \quad (11)$$

where  $j$  is the partial current density for  $\text{CH}_4$  formation,  $n$  is the number of electrons needed to reduce on  $\text{CO}_2$  molecule to  $\text{CH}_4$ , and 3 is the elementary charge.  $j$ ,  $n$ , and  $e$  are  $13 \text{ mA cm}^{-1}$ , 8, and

$1.602 \times 10^{16}$  C, respectively. Therefore, the TOF of  $\text{CH}_4$  for the CuPc catalyst at  $-1.06$  V vs RHE is  $0.39$  molecules sites $^{-1}$  s $^{-1}$ .

#### Method 5:

Foot of the wave analysis allows the use of measured CVs of catalytic reactions in order to determine TOF and TON, regardless of any side-effects such as substrate consumption, which may interfere with the obtained results at high current densities. We could extract TOF vs  $\eta$  Tafel plots for a specific homogeneous molecular catalyst.

A second order catalytic reaction rate ( $k$ ) could be calculated using the following relation:

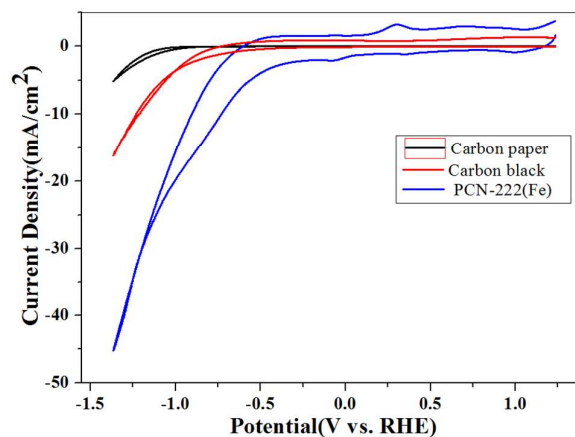
$$\frac{i}{i_p^0} = \frac{2.24 \sqrt{\frac{RT}{Fv}} 2k C_{\text{CO}_2}}{1 + \exp\left[\frac{F}{RT}(E - E_{\text{Fe 1/0}})\right]} \quad (12)$$

where  $i$  is the catalytic current under  $\text{CO}_2$  at a given applied potential  $E$ ,  $i_p^0$  is the current under  $\text{N}_2$  at the catalyst formal potential  $E_{\text{Fe 1/0}}$ .  $R$  is gas constant,  $T$  is temperature,  $F$  is Faraday constant, and  $v$  is CV scan rate.  $C_{\text{CO}_2}$  is  $0.23$  M in DMF.

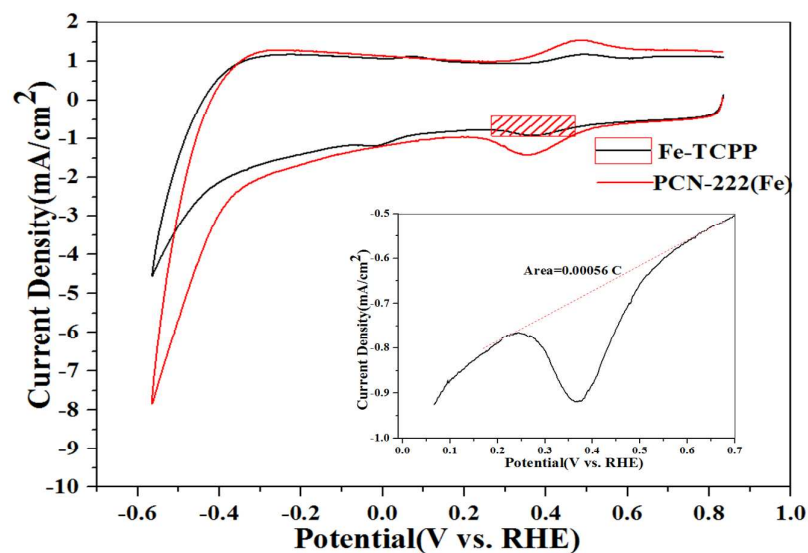
By plotting  $\frac{i}{i_p^0}$  vs  $1/1 + \exp\left[\frac{F}{RT}(E - E_{\text{Fe 1/0}})\right]$ , and fitting the early linear portion of the curve, one can calculate  $k$  from the curve's slope.

Then, TOF for each overpotential,  $\eta$ , could be obtained using:

$$\text{TOF} = \frac{2k}{1 + \exp\left[\frac{F}{RT}(E_{\text{CO}_2/\text{CO}} - E_{\text{Fe 1/0}} - \eta)\right]} \quad (13)$$



**Figure S9.** CVs of bare CP electrode, carbon black loaded on CP electrode and PCN-222 (Fe)/C loaded on CP in  $\text{CO}_2$ -saturated electrolyte in the potential range  $-1.4 \sim 1.2$  V vs RHE.



**Figure S10.** CVs of precursor of Fe-TCCP ligand ( $\Gamma = 2.89 \times 10^{-9} \text{ mol cm}^{-2}$ ), and PCN-222 (Fe)/C loaded on CP in  $\text{CO}_2$ -saturated electrolyte in the potential range  $-0.5 \sim 0.8 \text{ V}$  vs RHE.

The amount of surface-active Fe-TCCP sites is calculated by assuming a one-electron redox process:  $n = Q/F = 5.78 \times 10^{-9} \text{ mol}$ .

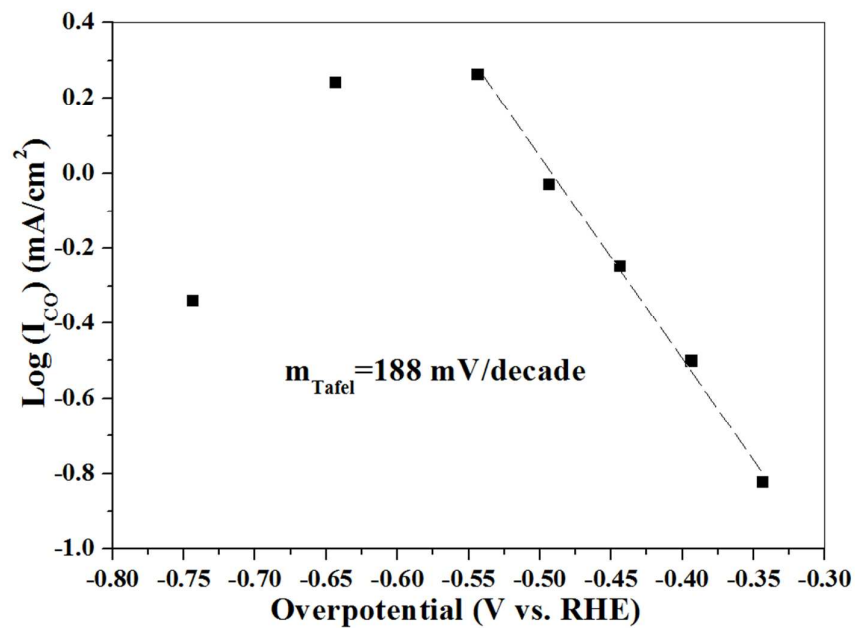
The total amount of Fe-TCCP is calculated as follows:  $n_{\text{total}} = m/M = 0.67/844.6 = 7.9 \times 10^{-7} \text{ mol}$ .

Then, the surface fraction of electrochemically active PCN-222(Fe) sites is determined as follows:

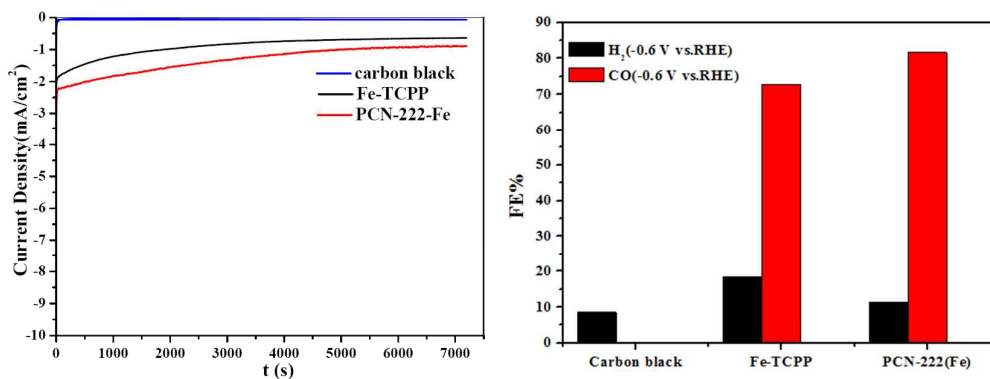
$$\chi = n/n_{\text{total}} = 0.73\%$$

**Table S2.** Summary of the chronoamperograms experiment parameters

<b>vs Ag/AgCl</b>	<b>-1.085</b>	<b>-1.135</b>	<b>-1.185</b>	<b>-1.235</b>	<b>-1.285</b>	<b>-1.385</b>	<b>-1.485</b>
<b>vs RHE/V</b>	<b>-0.45</b>	<b>-0.50</b>	<b>-0.55</b>	<b>-0.60</b>	<b>-0.65</b>	<b>-0.75</b>	<b>-0.85</b>
<b><math>\eta</math>/mV</b>	<b>344</b>	<b>394</b>	<b>444</b>	<b>494</b>	<b>544</b>	<b>644</b>	<b>744</b>
<b>Current density/mAcm<sup>-2</sup></b>	<b>0.23</b>	<b>0.46</b>	<b>0.71</b>	<b>1.15</b>	<b>2.330</b>	<b>3.46</b>	<b>4.08</b>
<b><math>Q/C</math></b>	<b>3.35</b>	<b>6.63</b>	<b>10.15</b>	<b>16.60</b>	<b>33.55</b>	<b>49.77</b>	<b>58.80</b>
<b><math>X_{H_2}\%</math></b>	<b>0.02</b>	<b>0.04</b>	<b>0.06</b>	<b>0.20</b>	<b>0.40</b>	<b>2.0</b>	<b>6.01</b>
<b><math>FE_{H_2}\%</math></b>	<b>4.70</b>	<b>4.75</b>	<b>4.65</b>	<b>9.48</b>	<b>11.27</b>	<b>38.01</b>	<b>80.49</b>
<b><math>X_{CO}\%</math></b>	<b>0.32</b>	<b>0.69</b>	<b>1.16</b>	<b>1.92</b>	<b>3.52</b>	<b>3.4</b>	<b>1.04</b>
<b><math>FE_{CO}\%</math></b>	<b>75.26</b>	<b>82.46</b>	<b>89.84</b>	<b>91.23</b>	<b>82.54</b>	<b>53.81</b>	<b>13.93</b>
<b><math>C_{MeOH/ppm}</math></b>	<b>0.198</b>	<b>0.394</b>	<b>0.509</b>	<b>0.192</b>	<b>0.50</b>	<b>1.57</b>	<b>0.986</b>
<b><math>FE_{MeOH}\%</math></b>	<b>6.42</b>	<b>6.45</b>	<b>5.45</b>	<b>1.26</b>	<b>1.62</b>	<b>3.44</b>	<b>1.82</b>
<b><math>C_{EtOH/ppm}</math></b>	<b>0.224</b>	<b>0.269</b>	<b>0.136</b>	<b>0.116</b>	<b>1.21</b>	<b>1.67</b>	<b>1.52</b>
<b><math>FE_{EtOH}\%</math></b>	<b>10.12</b>	<b>6.14</b>	<b>2.03</b>	<b>1.06</b>	<b>5.45</b>	<b>5.07</b>	<b>3.92</b>
<b><math>FE_{total}/\%</math></b>	<b>96.50</b>	<b>99.80</b>	<b>101.97</b>	<b>103.03</b>	<b>100.88</b>	<b>100.33</b>	<b>100.16</b>
<b><math>n_{CO}/mol</math></b>	<b><math>1.3 \times 10^{-5}</math></b>	<b><math>2.82 \times 10^{-5}</math></b>	<b><math>4.73 \times 10^{-5}</math></b>	<b><math>7.84 \times 10^{-5}</math></b>	<b><math>1.43 \times 10^{-4}</math></b>	<b><math>1.39 \times 10^{-4}</math></b>	<b><math>4.25 \times 10^{-5}</math></b>
<b>TON (<math>n_{co}/n_{pcn222}</math>)</b>	<b>16.7</b>	<b>36.2</b>	<b>60.6</b>	<b>100.7</b>	<b>183</b>	<b>178</b>	<b>54.4</b>
<b>TON<sub>corrected</sub> per site</b>	<b>400</b>	<b>858</b>	<b>1453</b>	<b>2414</b>	<b>4388</b>	<b>4268</b>	<b>1304</b>
<b>TOF/h<sup>-1</sup></b>	<b>8.35</b>	<b>18.1</b>	<b>30.3</b>	<b>50.4</b>	<b>91.5</b>	<b>89</b>	<b>27.2</b>
<b>TOF/s<sup>-1</sup></b>	<b>0.0023</b>	<b>0.0050</b>	<b>0.0084</b>	<b>0.0140</b>	<b>0.0254</b>	<b>0.0247</b>	<b>0.0075</b>
<b>TOF<sub>corrected</sub>/site<sup>-1</sup>·s<sup>-1</sup></b>	<b>0.055</b>	<b>0.120</b>	<b>0.201</b>	<b>0.336</b>	<b>0.609</b>	<b>0.592</b>	<b>0.180</b>



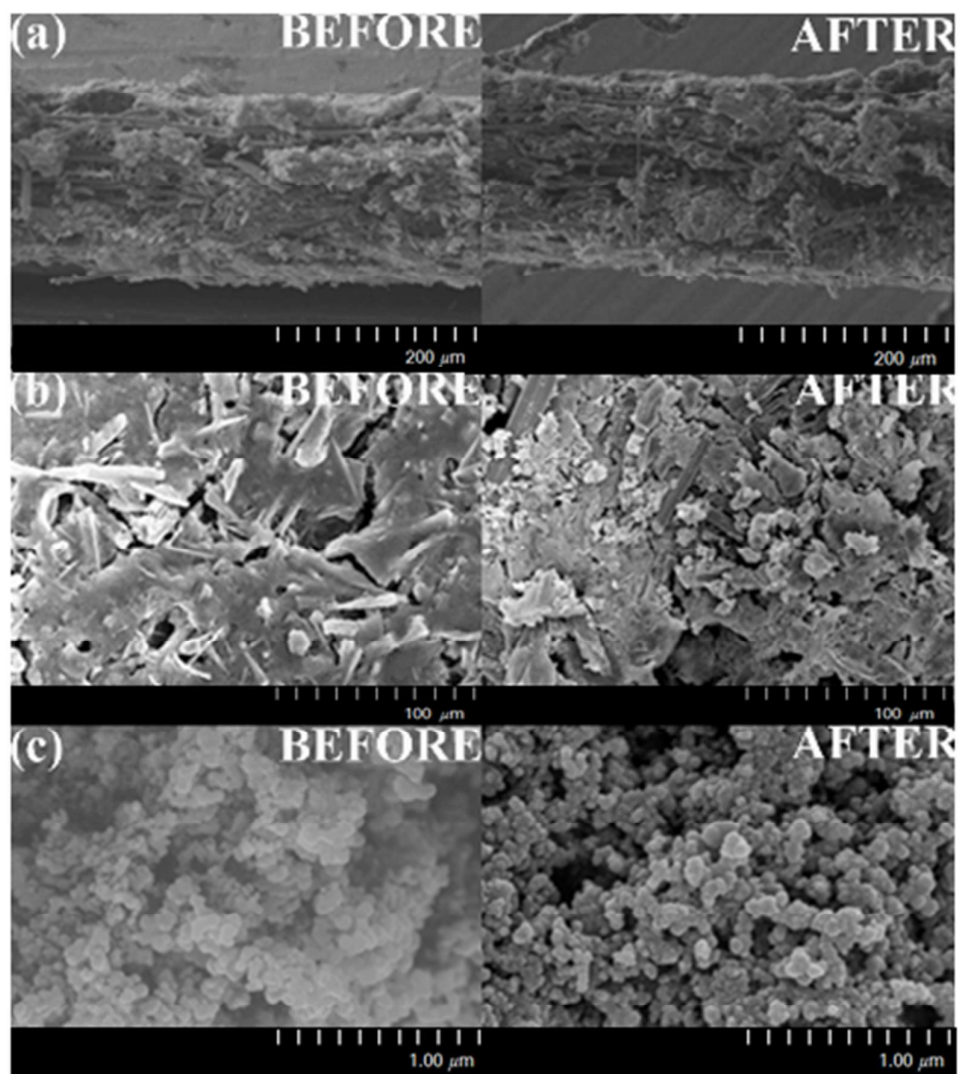
**Figure S11.** Plot of  $\log(I_{\text{CO}})$  vs  $\eta$  for CO production at varying potential, Tafel slope: 188 mV/decade.



**Figure S12.** Current density recorded for 2 h electrolyses (left) and FE analyses (right) at -0.60 V vs RHE using carbon black, Fe-TCPP/C and PCN-222 (Fe)/C, respectively, loaded on CP in CO<sub>2</sub>-saturated 0.5 M KHCO<sub>3</sub>.

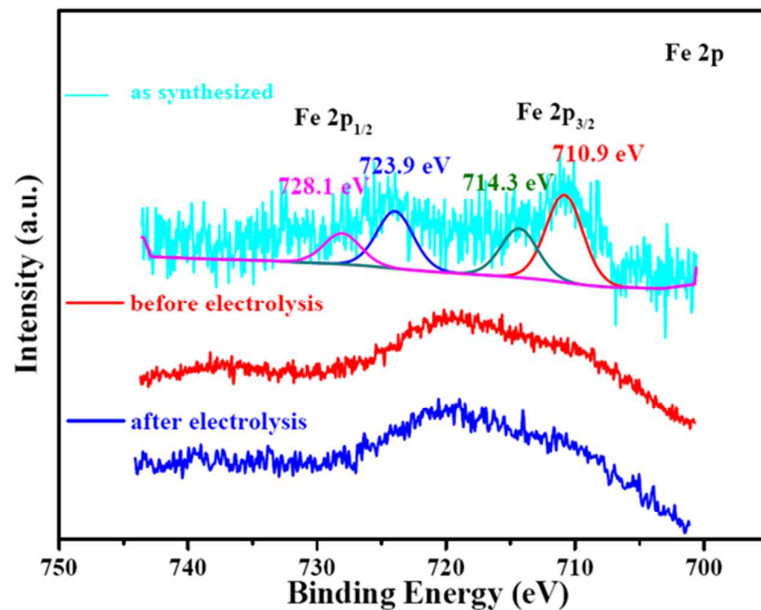
**Table S3.** List of the chronoamperograms experiment parameters for catalysts with different PCN-222(Fe): C ratios

PCN-222(Fe): C	1:3	1:2	1:1	2:1	3:1
$FE_{H_2}\%$	25.5	9.48	29.2	27.7	43.6
$FE_{CO}\%$	82.5	91.2	64.6	69.5	52.9
$X_{CO}\%$	1.94	1.92	1.29	1.20	0.69
$n_{CO}/mol$	$7.92 \times 10^{-5}$	$7.84 \times 10^{-5}$	$5.27 \times 10^{-5}$	$4.90 \times 10^{-5}$	$2.82 \times 10^{-5}$
$Q/C$	18.49	16.6	15.7	13.65	10.29
$j/mA\ cm^{-2}$	1.28	1.15	1.09	0.94	0.71
$Q_{CV}/C$	0.00026	0.00313	0.00070	0.00033	0.00030
$\Gamma/mol\ cm^{-2}$	$1.34 \times 10^{-9}$	$1.62 \times 10^{-8}$	$3.60 \times 10^{-9}$	$1.72 \times 10^{-9}$	$1.54 \times 10^{-9}$
$n_{(active\ pcn222)}/mol$	$2.68 \times 10^{-9}$	$3.24 \times 10^{-8}$	$7.20 \times 10^{-9}$	$3.44 \times 10^{-9}$	$3.08 \times 10^{-9}$
$n_{pcn222}/mol$	$5.83 \times 10^{-7}$	$7.78 \times 10^{-7}$	$1.16 \times 10^{-6}$	$1.56 \times 10^{-6}$	$1.75 \times 10^{-6}$
$\chi(n_{active}/n_{total})$	0.46%	4.17%	0.62%	0.22%	0.18%
TON( $n_{co}/n_{pcn222}$ )	135.8	100.7	45.4	31.4	16.1
TON <sub>corrected</sub> /site <sup>-1</sup>	29521	2414	7322	14272	8944

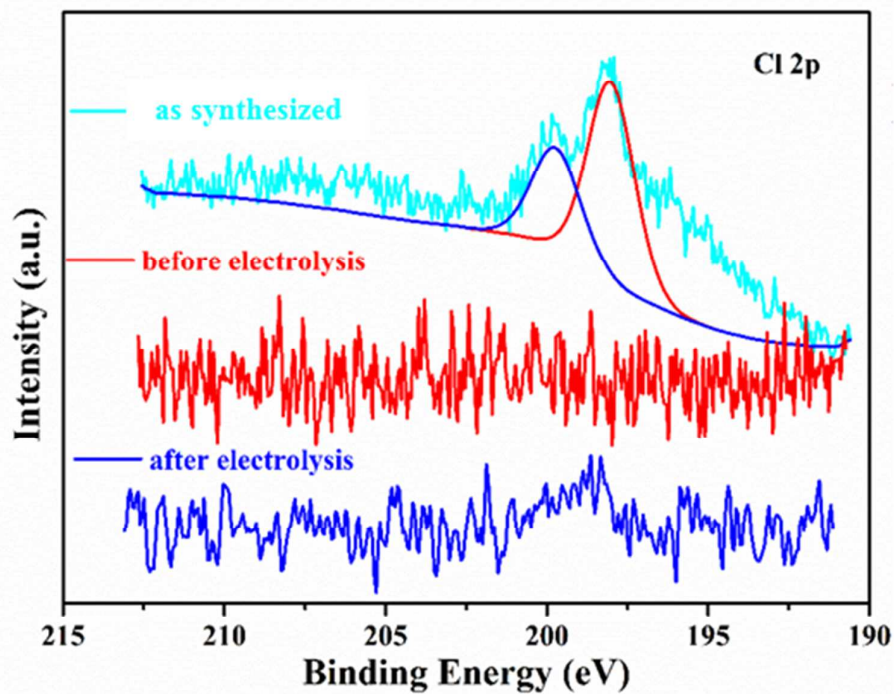


**Figure S13.** SEM images of the PCN-222(Fe)/C composite electrode before and after electrolysis in a side view (a) and top-view (b, c), respectively.

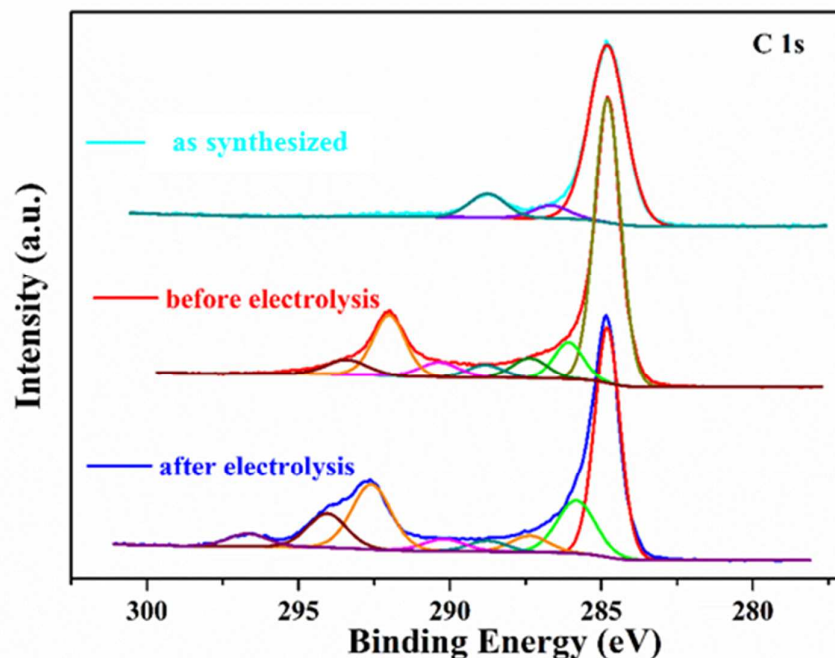




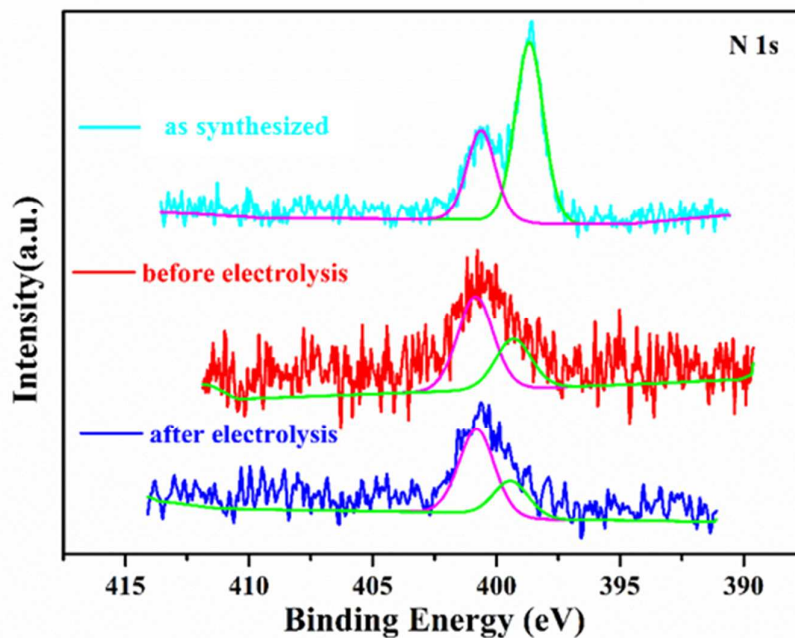
**Figure S14.** Fe2p core level spectra for as-synthesized PCN-222(Fe) and PCN-222(Fe)/C electrode loaded on carbon paper before and after electrolysis at  $-0.60$  V vs RHE for 2 h.



**Figure S15.** Cl2p core level spectra for as-synthesized PCN-222(Fe) and PCN-222(Fe)/C electrode loaded on carbon paper before and after electrolysis at  $-0.60$  V vs RHE for 2 h.



**Figure S16.** C1s core level spectra for as-synthesized PCN-222(Fe) and PCN-222(Fe)/C electrode loaded on carbon paper before and after electrolysis at  $-0.60$  V vs RHE for 2 h.



**Figure S17.** N1s core level spectra for as-synthesized PCN-222(Fe) and PCN-222(Fe)/C electrode loaded on carbon paper before and after electrolysis at  $-0.60$  V vs RHE for 2 h.

## References:

- (1) Costentin, C.; Drouet, S.; Robert, M.; Savéant, J. M. A Local Proton Source Enhances CO<sub>2</sub> Electroreduction to CO by a Molecular Fe Catalyst. *Science* **2012**, *338*, 90–94.
- (2) Morlanés, N.; Takanabe, K.; Rodionov, V. Simultaneous Reduction of CO<sub>2</sub> and Splitting of H<sub>2</sub>O by a Single Immobilized Cobalt Phthalocyanine Electrocatalyst. *ACS Catal.* **2016**, *6*, 3092–3095.
- (3) Hu, X.-M.; Salmi, Z.; Lillethorup, M.; Pedersen, E. B.; Robert, M.; Pedersen, S. U.; Skrydstrup, T.; Daasbjerg, K. Controlled Electropolymerisation of a Carbazole-Functionalised Iron Porphyrin Electrocatalyst for CO<sub>2</sub> Reduction. *Chem. Commun.* **2016**, *52*, 5864–5867.
- (4) Maurin, A.; Robert, M. Noncovalent Immobilization of a Molecular iron-based electrocatalyst on carbon electrodes for selective, efficient CO<sub>2</sub>-to-CO conversion in water. *J. Am. Chem. Soc.* **2016**, *138*, 2492–2495.
- (5) Weng, Z.; Jiang, J. B.; Wu, Y. S.; Wu, Z. S.; Guo, X. T.; Materna, K. L.; Liu, W.; Batista, V. S.; Brudvig, G. W.; Wang, H. L. Electrochemical CO<sub>2</sub> Reduction to Hydrocarbons on a Heterogeneous Molecular Cu Catalyst in Aqueous Solution. *J. Am. Chem. Soc.* **2016**, *138*, 8076–8079.
- (6) Hu, X. -M.; Rønne, M. H.; Pedersen, S. U.; Skrydstrup, T.; Daasbjerg, K. Enhanced Catalytic Activity of Cobalt Porphyrin in CO<sub>2</sub> Electroreduction upon Immobilization on Carbon Materials. *Angew. Chem. Int. Ed.* **2017**, *56*, 6468–6472.
- (7) Wu, Y. -S.; Jiang, J. -B.; Weng, Z.; Wang, M. -Y.; Broere, D. L. J.; Zhong, Y. -R.; Brudvig, G. W.; Feng, Z. -X.; Wang, H. -L. Electroreduction of CO<sub>2</sub> Catalyzed by a Heterogenized Zn–Porphyrin Complex with a Redox-Innocent Metal Center. *ACS Cent. Sci.* **2017**, *3*, 847–852.
- (8) Zhang, X.; Wu, Z. -S.; Zhang, X.; Li, L. -W.; Li, Y. -Y.; Xu, H. -M.; Li, X. -X.; Yu, X. -L.; Zhang, Z. -S.; Liang, Y. -Y. Wang, H. -L. Highly Selective and Active CO<sub>2</sub> Reduction Electrocatalysts Based on Cobalt Phthalocyanine/Carbon Nanotube Hybrid Structures. *Nature Commun.* **2017**, *8*, 14675.
- (9) Han, N.; Wang, Y.; Ma, L.; Wen, J. -G.; Li, J.; Zheng, H. -C.; Nie, K. -Q.; Wang, X. -X.; Zhao, F. -P.; Li, Y. -F.; Fan, J.; Zhong, J.; Wu, T. -P.; Miller, D. J.; Lu, J.; Lee, S. T.; Li, Y. -G. Supported Cobalt Polyphthalocyanine for High-Performance Electrocatalytic CO<sub>2</sub> Reduction. *Chem* **2017**, *3*, 652–664.
- (10) Weng, Z.; Wu, Y. -S.; Wang, M. -Y.; Jiang, J. -B.; Yang, K.; Huo, S. -J.; Wang, X. -F.; Ma, Q.; Brudvig, G. -W.; Batista, V. -S.; Liang, Y. -Y.; Feng, Z. -X.; Wang, H. -L. Active Sites of Copper-Complex Catalytic Materials for Electrochemical Carbon Dioxide Reduction. *Nat. Commun.* **2018**, *9*, 415–423.
- (11) Lin, S.; Diercks, C. S.; Zhang, Y. B.; Kornienko, N.; Nichols, E. M.; Zhao, Y.; Paris, A. R. Kim, D.; Yang, P.; Yaghi, O. M.; Chang, C. J. Covalent Organic Frameworks Comprising Cobalt Porphyrins for Catalytic CO<sub>2</sub> Reduction in Water. *Science* **2015**, *349*, 1208–1213.
- (12) Kornienko, N.; Zhao, Y.; Kley, C. S.; Zhu, C.; Kim, D.; Lin, S.; Chang, C. -J.; Yaghi, O. M.; Yang, P. Metal–Organic Frameworks for Electrocatalytic Reduction of Carbon Dioxide. *J. Am. Chem. Soc.* **2015**, *137*, 14129–14135.
- (13) Hod, I.; Sampson, M. D.; Deria, P.; Kubiak, C. P.; Farha, O. K.; Hupp, J. T. Fe-Porphyrin-Based Metal–Organic Framework Films as High-Surface Concentration,

Heterogeneous Catalysts for Electrochemical Reduction of CO<sub>2</sub>. *ACS Catal.* **2015**, 5, 6302–6309.

- (14) Costentin, C.; Drouet, S.; Robert, M.; Savéant, J.M. Turnover Numbers, Turnover Frequencies, and Overpotential in Molecular Catalysis of Electrochemical Reactions. Cyclic Voltammetry and Preparative-Scale Electrolysis. *J. Am. Chem. Soc.* **2012**, 134, 11235–11242.